Identification of poroelastic constants of deep argillaceous rocks. II: Inverse analysis

Brice Lecampion, Andrei Constantinescu

Identification of poroelastic constants of deep argillaceous rocks II: inverse analysis

Brice Lecampion & Andrei Constantinescu
Laboratoire de Mécanique des Solides, CNRS UMR 7649, Ecole Polytechnique, France

ABSTRACT: This paper discusses the identification of poroelastic constants from drained isotropic confinement and pulse test. Closed form solutions of the direct problem are obtained for a very thin specimen. The validity of these solutions for a realistic aspect ratio of the core is assessed by a comparison with a finite element model. The identification problem is solved by minimizing a least square functional using an explicit gradient and a Levenberg-Marquardt algorithm. Uniqueness of this inverse problem as well as the effect of noise on input data are fully discussed. The identification procedure is then applied to measurements performed on a deep argillaceous rock (argillite of Meuse Haute-Marne).

1 INTRODUCTION

This paper presents the quantitative identification of poroelastic parameters from laboratory tests. Our interest lies in the hydromechanical coupling in the isotropic confining and the pulse test performed on deep argillaceous rocks. The detailed description of the test is presented in the companion paper (see (Malinsky L. et al. 2002) for details and a qualitative interpretation of the tests) also presented at this conference. The aim of this paper is to discuss only the identification problem.

Next we shall interpret these tests within the framework of linear poroelasticity (Biot M.A. 1941; Detournay E. and Cheng A.H.D. 1993).

In the first part we shall discuss the closed form solution of the direct problems in the case of a very slender specimen and compare it with solutions obtained from finite element simulations. In this case, the solution of the pulse test is similar to the one obtained by (Hsieh P.A. et al. 1981) for the uncoupled case.

Next, the parameter identification problem is formulated as the minimization of a cost functional and solved using the direct differentiation of the closed form solution and a minimization algorithm.

Finally, we present the results obtained from tests performed on a deep argillaceous rock.

2 DIRECT PROBLEM

All tests are performed on a cylindrical core ($(r,z) \in [0,R] \times [0,L]$) under axisymmetric conditions.

In the general case, the poroelastic coupling does not allow to obtain a closed form solution for these particular configurations (Adachi J.I. and Detournay E. 1997). The problems are fully two-dimensional (see figure 1). This is due to the hydromechanical boundary condition on the radial surface: no hydraulic flux and an applied radial stress. Despite the apparent simplicity of these boundary conditions, the theory of linear poroelasticity imply non homogeneous hydromechanical fields in the core during the transient phase. (Adachi J.I. and Detournay E. 1997) have also shown that under the assumption of a very thin specimen ($m = R/L \ll 1$), the problems reduce to one dimension. We will derived closed form solutions in that particular case.

2.1 *Isotropic confinement test*

Boundary conditions

This test consists in the sudden application at $t = 0$ of an isotropic confining normal stress σ on all the specimen surfaces: $\boldsymbol{\sigma} \cdot \boldsymbol{n} = \sigma H(t)\boldsymbol{n}$, where $H(t)$ denotes the Heavyside function.

The radial surface of the sample remains undrained while the top and bottom surfaces are drained.

Solution in the slender case

In the case where $m = R/L \ll 1$, the stress and pore pressure fields are homogeneous. The evolution of pore pressure is therefore solution of the one dimensional diffusion equation:

$$\frac{\partial p}{\partial t} - D\frac{\partial^2 p}{\partial z^2} = -B\sigma\delta(t) \tag{1}$$

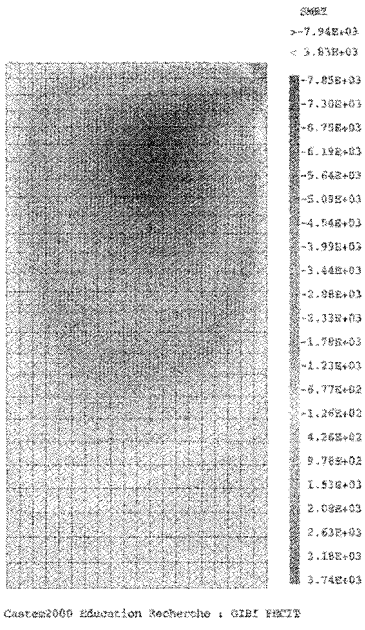

Figure 1. Contour of the shear component of the stress tensor during the transient phase of an isotropic confining test. Finite element model , axisymmetry, poroelastic coupling.

$$p(L,t) = p(0,t) = 0 \quad p(z,0) = 0 \tag{2}$$

where $\delta(t)$ is the Dirac distribution. B $[\cdot]$[1] is the Skempton dimensionless coefficient. The diffusivity D $[L^2T^{-1}]$ is given by (Detournay E. and Cheng A.H.D. 1993):

$$D = kM\frac{K}{K_u} \tag{3}$$

where:

- k $[M^{-1}L^3T]$ is the hydraulic conductivity of the specimen related to the intrinsic permeability κ $[L^2]$: $k = \frac{\kappa}{\mu f}$, μf is the fluid viscosity,
- M $[ML^{-1}T^{-2}]$ is the Biot Modulus,
- K $[ML^{-1}T^{-2}]$ is the drained bulk modulus,
- K $[ML^{-1}T^{-2}]$ is the undrained bulk modulus.

We now use the following dimensionless variables:

$$t^* = \frac{Dt}{L^2} \quad z^* = \frac{z}{L} \quad \Pi = \frac{p}{\sigma} \tag{4}$$

The dimensionless pore pressure is given by (Carslaw H.S. and Jaeger J.C. 1959):

$$\Pi(z^*,t^*) = -B\int_0^1 h(z^*,t^*;\xi)\,d\xi = -B\mathcal{K}(z^*,t^*) \tag{5}$$

[1] Between brackets $[\cdot]$ we indicate the physical dimensions of the parameters

with $\mathcal{K}(z;t)$:

$$\mathcal{K}(z^*,t^*) = \frac{4}{\pi}\sum_{n=1}^{\infty}\exp(-4n^2\pi^2t^*)\sin(2n\pi z^*) \tag{6}$$

In this case, the linear poroelastic constitutive equations in cylindrical coordinates (Biot M.A. 1941; Detournay E. and Cheng A.H.D. 1993) are written as follows:

$$\varepsilon_{zz} = \frac{\partial u_z}{\partial z^*} = \frac{\sigma}{3K}(1 + b\Pi(z^*,t^*)) \tag{7}$$

$$\varepsilon_{rr} = \frac{\partial u_r}{\partial r}\varepsilon_{\theta\theta} = \frac{u_r}{r} = \frac{\sigma}{3K}(1 + b\Pi(z^*,t^*)) \tag{8}$$

where $b[\cdot]$ denotes the Biot coefficient.

From $bB = K_u - K/K_u$, one obtains the overall axial, and the radial displacement at the middle of the specimen. These displacements are recorded during an experimental test.

$$\frac{u_z(1,t^*)}{L} = \frac{\sigma}{3K}\left(1 - \frac{K_u - K}{K_u}\mathcal{I}(1,t^*)\right) \tag{9}$$

$$\frac{u_r(1/2,t)}{R} = \frac{\sigma}{3K}\left(1 - \frac{K_u - K}{K_u}\mathcal{K}(1/2,t)\right) \tag{10}$$

$\mathcal{I}(1,t^*) = \int_0^1 \mathcal{K}(\xi,t^*)\,d\xi$ is given by the following series:

$$\mathcal{I}(1,t^*) = \frac{2}{\pi^2}\sum_{n=1}^{\infty}\exp(-n^2\pi^2t^*)\left(\frac{1}{n} - \frac{\cos n\pi}{n}\right)^2 \tag{11}$$

The series (7) and (11) are precisely estimated even for small value of t^* when keeping the 10 first terms of the series.

2.2 *Pulse test*

Boundary conditions

Prior to the beginning of the test, the sample is in an homogeneous and isotropic stress state. The applied stress is kept constant during the test. The hydraulic boundary conditions are:

- no flux on the radial surfaces
- the pore pressure on the boundary Γ_{re} between the reservoir and the specimen is equal to the fluid pressure of the reservoir p_r. The pore pressure does not vary spatially on Γ_{re}:

$p(\mathbf{r},t) = p_r(t)$ on Γ_{re} at all time instants.

At $t = 0$, the fluid pressure in the reservoir p_r is suddenly increased to the so called injection value p_0. Taking into account the reservoir stiffness C_r, we can write the fluid mass balance in the reservoir as:

$$\int_{\Gamma re} -\boldsymbol{k}\nabla p(\mathbf{r},t)\cdot\boldsymbol{n}\,d\Gamma = \frac{1}{C_r}\frac{dp_r(t)}{dt} \tag{12}$$

Solution in the slender case

In the slender case, the diffusion equation is independent of the mechanical state. Its solution is therefore similar to the classical one given by (Hsieh P.A. et al. 1981).

We use a similar set of dimensionless variables as for the isotropic test. The dimensionless pore pressure is here scaled using the injection pressure p_0: $\Pi = \frac{p}{p_0}$. Another dimensionless parameter related to the constitutive parameters is introduced:

$$\gamma = \frac{MK}{C_r K_u \pi R^2 L} \tag{13}$$

The diffusion equation together with the initial and boundary conditions give the following system of equations:

$$\begin{aligned} \frac{\partial \Pi}{\partial t^*} - \frac{\partial^2 \Pi}{\partial z^{*2}} &= 0 \\ \gamma \frac{d\Pi}{dt^*} - \frac{\partial \Pi}{\partial z^*} &= 0 \quad \text{in } z^* = 0 \\ \frac{\partial \Pi}{\partial z^*}(1/2, t^*) &= 0 \\ \Pi(0,0) = 1 \quad \Pi(z^*, 0) &= 0 \end{aligned}$$

The solution in the Laplace domain is given by:

$$\overline{\Pi}(z^*, s) = \frac{\gamma \cosh\left(\sqrt{s}(1/2 - z^*)\right)}{\gamma s \cosh\left(\frac{\sqrt{s}}{2}\right) + \sqrt{s} \sinh\left(\frac{\sqrt{s}}{2}\right)} \tag{14}$$

No simple analytical expression of the inverse Laplace transform exists for the last expression. The inversion is performed numerically using Stehfest algorithm (Cheng A.H-D et al. 1994).

2.3 *Consistency of the closed form solutions*

A series of axisymmetric finite element simulations using the object oriented code have been performed for different aspect ratios.

For both configurations, the comparison is done using the following set of parameters :

$$K = 6\,GPa \quad K_u = 7.1\,GPa \quad G = 4\,GPa$$
$$M = 4\,GPa \quad D = 0.7 \times 10^{-3}\,m^2 \cdot s^{-1}$$

The relative error between the numerical and the closed form solution for different aspect ratio is displayed on figure 2 for the isotropic confinement test. We note, as expected, that the error is only significant during the transient phase. A similar pattern can be observed for the pulse test.

For the aspect ratio of our specimen ($m = 0.25$) the coupling effect is negligible, i.e. the relative error ε on the axial strain is at most of 1%.

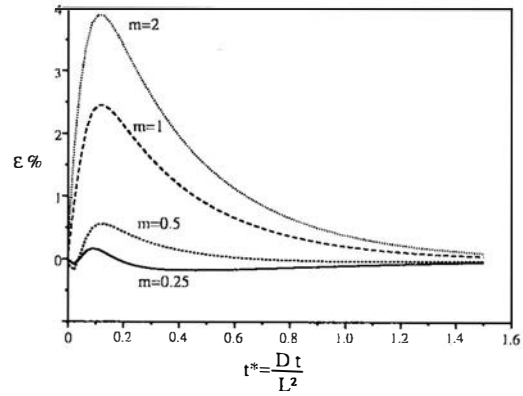

Figure 2. Relative error on the axial strain between the closed form and the coupled finite element solution for different aspect ratio $m = R/L$.

A series of computations for different value of G did not show a major influence on this error.

In the case of a thin specimen, it is therefore possible to use the closed form solution without losing any accuracy. In doing so, a large amount of computation time is saved compared to finite element simulations.

3 INVERSE PROBLEM

3.1 *Formulation*

We want to identify a certain set of parameters $\boldsymbol{c}$ from the recorded displacements or reservoir pressure.

- For the *isotropic confinement test*, $\boldsymbol{c} = (K, K_u, D)$ will be identified from the evolution of the axial ($u_z(t)$) and/or radial ($u_r(t)$) displacements.
- In the case of the *pulse test*, $\boldsymbol{c} = (\gamma, D)$ will be identified from the recorded reservoir pressure $p_r(t)$ decay.

The estimation of unknowns parameters from measurements is an inverse problem. For the configurations under study, algebraic manipulations of expression (10) and (14) permit to prove that the knowledge of the history of measurements uniquely determines the set of parameters $\boldsymbol{c}$. Details of this proof will not be presented here.

This uniqueness result does not guarantee the stability of the inverse problem, i.e.: a small variation in input data can induce a large variation of the identified parameters.

3.2 *Identification procedure*

In spite of the knowledge the closed form solution, we do not possess an analytical expression directly relating the unknown parameters to the measurements.

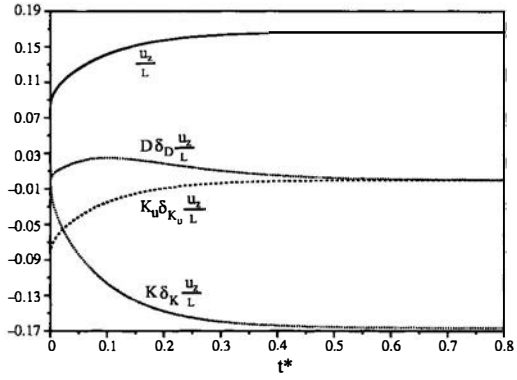

Figure 3. Dimensionless total axial displacement u_z/L and associated sensitivity coefficient on K, K_u and D during an isotropic confinement test.

The solution of the identification problem will be based on the minimization of a cost functional measuring the distance between predictions and measurements.

$$\mathcal{J}(\boldsymbol{c}) = \frac{1}{2}\sum_{i=1}^{n}(f(\boldsymbol{c}, t_i) - f_{meas}(t_i))^2 \qquad (15)$$

n is the number of measurements recorded during the test. f denotes the measured quantity : radial or axial displacement for the confinement test, reservoir pressure for the pulse test.

The minimization of this functional is performed using a Levenberg-Marquardt gradient based algorithm (see (Gill P.E. et al. 1982) for details).

As displayed in figure 4, the cost functional can be considered as convex in the explored region and does not have multiple minima. This assesses the choice of a gradient based algorithm.

The closed form (semi explicit) solutions are differentiated with respect to the constitutive parameters in order to obtain the gradient of the cost functional. The sensitivity coefficient (partial derivatives with respect to constitutive parameters) on the axial displacement in the case of the isotropic confinement test are displayed on figure 3. We can remark that the experimental response contains information on the undrained modulus at early time. At large time, the displacement only depends on the drained modulus. The sensitivity on the diffusivity coefficient is maximum during the transient phase.

3.3 *Effect of noise and initial guess*

In order to investigate the stability of the identification problems related to the isotropic confinement test and pulse test, we have simulated a series of measurements with a so called optimum set of parameters $\boldsymbol{c}_{opt}$. The identification is then performed for different

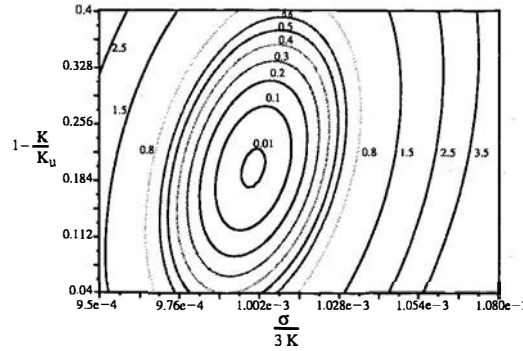

Figure 4. Contour of the cost functional in the plane $(1-K/K_u,\ \sigma/3K)$ in the case of recorded axial displacement.

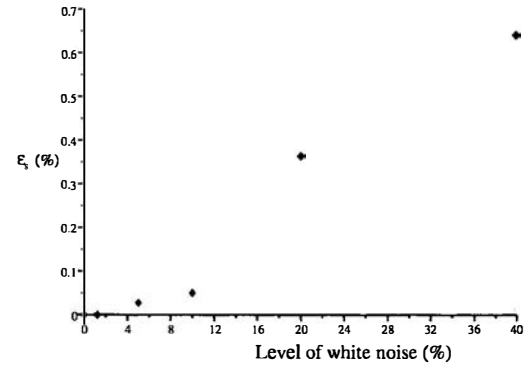

Figure 5. Stability of the identification (isotropic confinement test). Evolution of ε_s with the level of white noise.

initial guesses. The optimum parameters are always retrieved in few iterations.

The effect of a white noise on simulated data has also been studied. From the identified parameters $\boldsymbol{c}_{noise}$, we can compute the following stability estimator:

$$\varepsilon_s = \frac{\|\boldsymbol{c}_{noise} - \boldsymbol{c}_{opt}\|}{\|\boldsymbol{c}_{opt}\|} \qquad (16)$$

One can see on figure 5 the astonishing stability of the identification problem with respect to white noise. Of course, in the case of real measurements, if the poroelastic model is not adequate, the identification may be more unstable.

4 RESULTS AND DISCUSSION

Next, the experimental tests qualitatively discussed in (Malinsky L. et al. 2002) are used to identify the poroelastic constants.

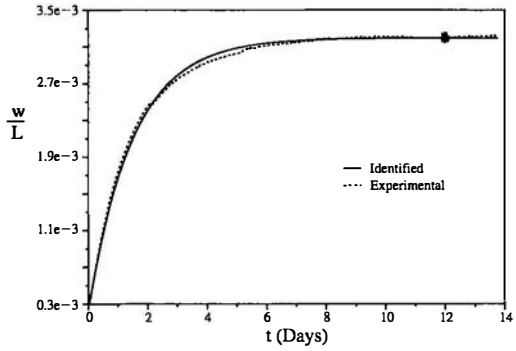

Figure 6. Experimental and identified response (axial strain) to an isotropic confinement test performed on argillite of Meuse Haute-Marne.

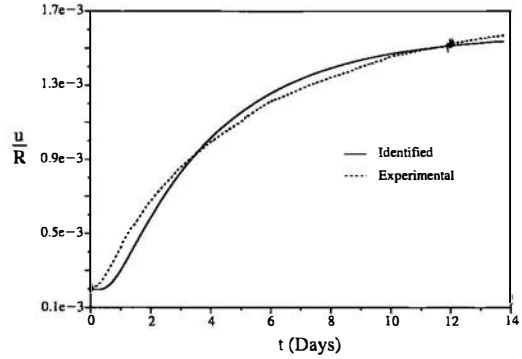

Figure 7. Radial strain (isotropic confinement).

Table 1. Estimation of the intrinsic permeability for different values of the Biot modulus with $K = 1.04\,GPa$, $K_u = 9.82\,GPa$ and $D = 4.02 \times 10^{-9}\,m^2 \cdot s^{-1}$. Identification performed on axial displacement.

M (GPa.)	$\kappa\ (m^2)$
5	7.5×10^{-21}
10	3.7×10^{-21}
15	2.5×10^{-21}

4.1 *Isotropic confinement*

The identification performed using *only* the axial displacement of the isotropic drained consolidation on sample *n*°2 gives a perfect fit (figure 6). The same parameters are obtained for different initial guesses:

$$K = 1.04\,GPa; \quad K_u = 9.82\,GPa;$$
$$D = 4.02 \times 10^{-9}\,m^2 s^{-1}$$

It is also possible to compute the intrinsic permeability for different estimated value of the Biot's modulus M. Table 1 presents the results. An intrinsic permeability of the order of magnitude of $1 \times 10^{-21} m^2$ matches known values for a damage argillite.

The identification performed using *only* the radial displacement at the middle of the specimen gives the following parameters:

$$K = 2.12\,GPa; \quad K_u = 16.9\,GPa;$$
$$D = 1.74 \times 10^{-9}\,m^2 \cdot s^{-1}$$

The important anisotropy between axial and radial displacement can be explained by the high level of damage of the sample (see (Malinsky L. et al. 2002)).

A close inspection of figure 7 shows on the one hand that the measured radial displacement has not reach its asymptotic value after 15 days, whether the computed one tends to its asymptot. On the other hand, at early time the measured initial delay due to the diffusion process is rather small when compared to the computed one. These discrepancies are an effect of the simple poroelastic model, not an aterfact of the identification.

It is possible to quantify the degree of confidence on the identified parameters. The sensitivity coefficient at the optimum point provides an information on the correlation between the parameters (Tarantola A. 1987). The correlation between the drained bulk modulus and the diffusivity is large ($C_{KD} = 0.85$). These can be explained by the influence of other physical phenomena (swelling, chemical reaction).

We can report that the correlations obtained from axial displacement are very small, as one could expect with independently identified parameter.

4.2 *Pulse test*

The identification method has also been applied to a pulse test conducted in 1999 on a slightly different argillite (Coste F. et al. 1999). The experimental as well as the identified response are displayed on figure 8.

Table 2 presents the identified parameters for different values of the initial guess and the correlation between the identified parameters. The high value of correlation can be explained by the lack of data at large time or by the discrepancy between the experimental and identified response during the transient phase.

It is important to remark that the exact value of the reservoir stiffness C_r was not precisely known at this time. Table 3 display the value of the coefficient MK/K_u and of the intrinsic permeability κ for a range of acceptable values of C_r.

We can notice that the obtained values matches standard physical values for an argillite.

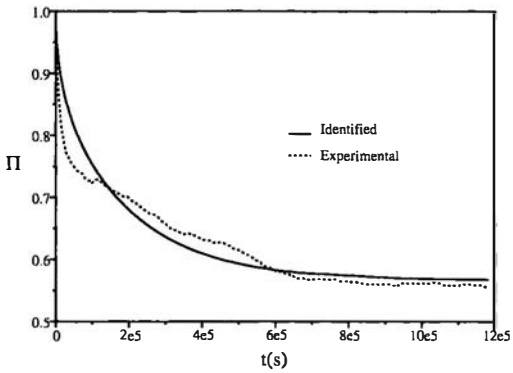

Figure 8. Pulse test on a argillite from Meuse Haute-Mame.

Table 2. Pulse test on a argillite (1999). Results of the identification for different initial guess.

	γ	$\frac{D}{L^2}\ s^{-1}$	$\mathcal{J}$	$C_{\gamma D}$
initial	0.8	1×10^{-6}	0.216	
final	0.6531	3.186×10^{-7}	0.09084	0.8373
initial	1.8	1×10^{5}	2.872	
final	0.653	3.19×10^{-7}	0.09084	0.8372
initial	0.1	1.5×10^{-7}	16.65	
final	0.6537	3.195×10^{-7}	0.0906	0.8381

Table 3. Estimation of the coefficient MK/K_u and the intrinsic permeability for different values of the reservoir compressibility. $\gamma = 0.653, D = 3.53E-9\ m^2 \cdot s^{-1}$

$C_r(GPa.m^{-3})$	$\frac{MK}{K_u}\ (MPa)$	$\kappa\ (m^2)$
8×10^7	15.536	2.27×10^{-22}
4×10^7	7.76	4.54×10^{-22}
1.33×10^7	2.58	2.654×10^{-21}

5 CONCLUSIONS

In this communication, we have discussed the identification of several poroelastic parameters from drained isotropic confinement test and pulse test. We have shown that for specimen with an aspect ratio $R/L \ll 0.25$, we can use the closed form solutions obtained for a very thin specimen. This permits to speed up the identification procedure.

The proposed identification method has shown to provide robust and efficient solution to this inverse problem.

The identified values of the constitutive parameters for the argillite of Meuse Haute-Marne are within the expected range. The mismatches between the model and the experiment show on the one hand that the samples were damaged prior to the test and on the other hand that probably others physical phenomena (swelling, chemical reaction ...) should also be taken into account.

We can conclude that the combination of the drained isotropic confinement and the pulse test permits a complete identification of the poroelastic parameters with the exception of the shear modulus. The methodology presented here can be extended to the identification of others porous material.

ACKNOWLEDGMENTS

We would like to thank Pr. E. Detournay and Dr J. I. Adachi for the benefit of useful discussion, Pr P. Bérest for a careful review of the companion papers. This research is funded by the French agency for radioactive waste management (ANDRA) through the PhD grant of B.L.

REFERENCES

Adachi J.I. and Detournay E. (1997). A poroelastic solution of the oscillating pore pressure method to measure permeabilities of "tight" rocks. *Int. J. Rock Mech. & Min. Sci. 34*(3–4). Paper No. 062.

Biot M.A. (1941). General theory of three-dimensional consolidation. *Journal of Applied Physics 12*, 155–164.

Carslaw H.S. and Jaeger J.C. (1959). *Conduction of heat in solids.* Oxford science publications.

Cheng A.H-D., Sidauruk P., and Abousleiman Y. (1994). Approximate inversion of the laplace transform. *The Mathematica Journal 4*(2), 76–82.

Coste F., Bounenni A., Chanchole S., and Su K. (1999). A method for measuring mechanical, hydraulic and hydromechanical properties during damaging in materials with low permeability. In *Int. Workshop on, Ecole des Mines de Paris, France.*

Detournay E. and Cheng A.H.D. (1993). *Fundamentals of Poroelasticity,in Comprehensive Rocks Engineering,* Volume 2, Chapter 5, pp. 113–171. Pergamon Press, London.

Gill P.E., Murray W., and Wright M.H. (1982). *Practical optimization.* Academic Press.

Hsieh P.A. , Neuzil C.E., Bredehoeft J.D., and Silliman S.E. (1981). Transient laboratory method for determining the hydraulic properties of tight rocks- part i: Theory. *Int. J. Rock Mech. & Min. Sci 18*, 245–252.

Malinsky L., Chanchole S., and Coste F. (2002). Identification of poroelastic constants of deep argillaceous rocks. 1: Experimental set up and qualitative analysis. In 2nd *Biot conference on Poromechanics, Grenoble, France.*

Tarantola A. (1987). *Inverse Problem Theory.* Elsevier.